NOTES AND CORRESPONDENCE

A Study of the Antarctic Surface Energy Budget Using a Polar Regional Atmospheric Model Forced with Satellite-Derived Cloud Properties

MICHAEL J. PAVOLONIS

Cooperative Institute for Meteorological Satellite Studies, University of Wisconsin—Madison, Madison, Wisconsin

JEFFREY R. KEY

Office of Research and Applications, NOAA/NESDIS, Madison, Wisconsin

JOHN J. CASSANO

Cooperative Institute for Research in Environmental Sciences, University of Colorado, Boulder, Colorado

7 February 2003 and 8 September 2003

ABSTRACT

Cloud properties from the newly extended Advanced Very High Resolution Radiometer (AVHRR) Polar Pathfinder (APP-x) dataset were incorporated into the atmospheric component of the Arctic Regional Climate System Model (ARCSyM) in order to improve the simulation of the Antarctic surface energy balance. A method for using the APP-x cloud properties in 48-h model simulations is presented. In the experiments, the model cloud fields were altered via the water vapor mixing ratio using cloud properties from the APP-x dataset. Significant improvements in monthly mean downwelling longwave radiation at the surface were observed relative to surface measurements. In the austral summer, the use of the APP-x dataset resulted in improvements as large as 30 W m^{-2} at the South Pole when compared to model results without APP-x clouds. However, only a very small improvement was seen in the turbulent heat fluxes and the surface temperature. It was also found that the satellite data can be used to shorten the model ''spinup'' time and may be useful in model initialization for short duration forecasts.

1. Introduction

An accurate parameterization of clouds is critical for producing accurate surface energy balance simulations in the Antarctic with global and regional climate/forecast models. For example, Hines et al. (1999) found that the monthly mean downwelling longwave flux at the surface over the Antarctic continent was up to 50 W m^{-2} too small in the National Centers for Environmental Prediction (NCEP) Medium-Range Forecast (MRF) Model simulations because of underestimated cloud amounts. King and Connolley (1997) found errors as large as 20 W m^{-2} in the monthly mean downwelling longwave radiation over the Antarctic continent in the U.K. Meteorological Office Unified Climate Model. Lubin et al. (1998) showed that differences in the parameterization of the microphysical properties of Antarctic clouds in global climate model (GCM) simulations can lead to dramatic changes in the regional dynamics in the Antarctic. Regional changes in the dynamics within the South Polar region were shown to cause changes in the zonal winds, meridional mass flux, and latent heat release in the Tropics and midlatitudes of the Northern Hemisphere. Thus it is important to accurately simulate cloud amount, cloud location, and cloud microphysical properties in the Antarctic. Furthermore, as King and Connolley (1997) assert, it is important for a model to not only accurately simulate surface temperature but the individual components of the surface energy budget as well, that is, shortwave and longwave radiative fluxes, sensible and latent heat fluxes, and the conductive flux. These components define the surface energy budget as

$$L_{\downarrow} - L_{\uparrow} + (1 - \alpha)S_{\downarrow} + H_S + H_L + G = 0, \quad (1)$$

where $L_{\downarrow}$ is the downwelling longwave flux, $L_{\uparrow}$ is the upwelling longwave flux, $(1 - \alpha)S_{\downarrow}$ is the absorbed (net) shortwave flux (α is the surface albedo and $S_{\downarrow}$ is the downwelling shortwave flux), H_S is the sensible heat

Corresponding author address: Michael Pavolonis, University of Wisconsin—Madison, 1225 West Dayton St., Madison, WI 53706.
E-mail: mpav@ssec.wisc.edu

flux, H_L is the latent heat flux, and G is the conductive flux through the ice/snow pack. Radiative fluxes are always taken to be positive, and the other components are positive when directed toward the surface.

In this paper we describe a modeling study designed to improve the estimation of the Antarctic surface energy budget. Water vapor amounts in an atmospheric model are adjusted during the model simulations such that the horizontal and vertical location of clouds in the model more closely match satellite observations, under the assumption that our satellite-derived clouds are more realistic than modeled cloud fields. Modeled radiative and turbulent heat fluxes are validated against surface measurements at the South Pole and over the Ross Ice Shelf for 1987.

2. Datasets and model

The standard Advanced Very High Resolution Radiometer (AVHRR) Polar Pathfinder (APP) products include spectral radiance, viewing and illumination geometry, three cloud masks, and clear-sky surface temperature and albedo sampled at a 5-km resolution into two daily composite images covering both polar regions (Meier et al. 1997; Maslanik et al. 1998, 1999). The APP dataset has been expanded to include cloud optical depth, cloud-top pressure, cloud-top temperature, cloud phase, cloud particle effective radius, radiative fluxes, and cloud forcing on a 25-km scale, subsampled from 5-km pixels (hereinafter called ''APP-x''). Clouds are taken to be composed of liquid water droplets or ice particles; mixed-phase clouds are not considered. However, the consideration of mixed-phased clouds should be secondary to more accurately simulating the location of clouds. The composite times are 0200 and 1400 local solar time (LST), with most of the observations falling within 1 h of those times. Surface temperature is calculated with a split-window infrared algorithm. Surface albedo retrieval for clear and cloudy skies employs corrections for anisotropic reflectance and atmospheric effects (Key et al. 2001). Cloud detection is done with a variety of spectral and temporal tests optimized for high-latitude conditions. APP-x monthly mean cloud amounts were found to be within 10% of surface observations at Neumayer Station in Antarctica during the summer, with the APP-x cloud amounts as much as 25% greater in the winter when the surface observations tend to be underestimated (Pavolonis 2002). At the South Pole, the APP-x monthly mean cloud amounts were generally within 15% of surface observations during the sunlit months. Cloud particle phase uses near-infrared reflectances (daytime) and infrared brightness temperature differences to separate ice and liquid (''water'') clouds (Key and Intrieri 2000). Cloud optical depth and particle effective radius retrievals use absorbing and nonabsorbing wavelengths, where the absorbing wavelength is more sensitive to particle size, and the nonabsorbing wavelength is more sensitive to optical depth. The cloud optical depth and particle effective radius retrieval algorithms are described in detail in Gultepe et al. (2003). Validation efforts are also discussed in Gultepe et al. (2003).

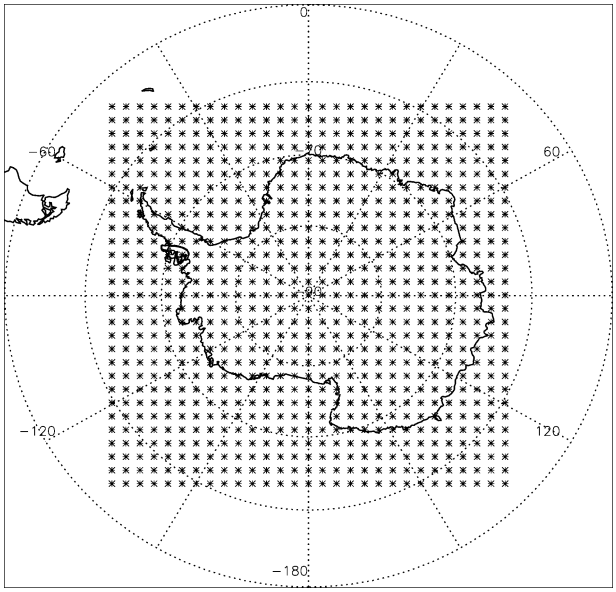

FIG. 1. The ARCSyM 200-km horizontal grid used for all Antarctic experiments.

APP-x data were used to force the Arctic Regional Climate System Model (ARCSyM) (Lynch et al. 1995; Bailey and Lynch 2000a,b). ARCSyM has as its heritage the National Center for Atmospheric Research (NCAR) Regional Climate Model Version 2 (Giorgi et al. 1993a,b), which utilizes a hydrostatic primitive equation atmospheric model. The ARCSyM, however, is specifically designed to simulate the polar atmosphere. The ARCSyM staggered ''Arakawa B'' (Arakawa and Lamb 1977) horizontal grid was set to a resolution of 200 km for all model simulations (Fig. 1), a resolution chosen for computational efficiency. The horizontal model domain consists of 31 by 31 grid points and covers the entire Antarctic continent and adjacent oceans. In addition, 23 terrain-following vertical sigma levels, with the greatest resolution in the boundary layer, were used for all model simulations. The lowest sigma level used is 0.99, which is about 40 m above the ground. The lowest level used in the simulations is similar to the lowest height used in operational forecast models. The pressure at the model top was set to 50 mb. The model was initialized and forced at the lateral boundaries with European Centre for Medium-Range Weather Forecasts (ECMWF) operational analyses (Trenberth 1992). The lateral boundaries were forced using a sponge boundary condition every time step (60 s). A sponge boundary condition is also applied at the top boundary.

The NCAR Community Climate Model Version 2 (CCM2) shortwave radiation scheme (Briegleb 1992), the Rapid Radiative Transfer Model (RRTM; Mlawer et

al. 1997) longwave radiation model, the planetary boundary layer scheme of Holtslag et al. (1990), and the NCAR Land Surface Model (LSM; Bonan 1996) were employed for all simulations. An implicit moisture scheme (Giorgi et al. 1993a) was used because Hines et al. (1997) showed that the more comprehensive explicit moisture scheme of Hsie et al. (1984) did not perform well in the Antarctic. The cloud scheme predicts the mixing ratio of the cloud-sized particles. These particles are identified as liquid or ice phase based on a threshold temperature of 258.16 K. These mixing ratios are used in the radiation code to determine the emissivity of the cloudy grid cells. Radiative transfer calculations are performed every 15 min. Convective processes were not included, but this should have a minimal impact on the results because significant convection occurs relatively infrequently in the Antarctic, especially over the Antarctic continent. The thermodynamic sea ice model of Parkinson and Washington (1979), with modifications by Schramm et al. (1997), was used. A dynamic sea ice model was not utilized because sea ice concentration was initialized and updated every day at 0000 UTC from the 25-km Scanning Multichannel Microwave Radiometer (SMMR) sea ice concentration product prior to about July 1987 and from the Special Sensor Microwave Imager (SSM/I) sea ice concentration product (Comiso 2002) thereafter.

3. Procedure

The resolution of the APP-x dataset was first converted from 25 to 200 km to match the ARCSyM grid. This was accomplished by averaging the cloud optical depth, cloud particle size, and cloud-top pressure for cloudy pixels from the APP-x dataset in a given ARCSyM grid cell (Fig. 1). Cloud thermodynamic phase and cloud amount require a different treatment, where the 200-km resolution cloud phase was taken to be the mode of the 25-km phase retrievals (either water or ice) that fall within in each ARCSyM grid cell, and the cloud fraction was the number of cloudy APP-x pixels divided by the total number of pixels within each ARCSyM grid cell. The geometric cloud thickness for each 200-km grid cell was calculated as the cloud visible optical depth multiplied by the extinction coefficient, which is based on the cloud particle size and phase. If all of the 25-km APP-x values within a given grid cell were missing, then the grid cell value was also missing. This rarely occurred. Surface temperature from the APP-x dataset was also averaged to match the ARCSyM 200-km grid, and any missing grid cell values were filled using a kriging procedure. If an entire day of surface temperature data was missing, then linear interpolation is used to fill in the missing day. The APP-x surface temperatures were used to initialize and update the ARCSyM sea surface temperatures (SSTs) at 0000 UTC in model time. Sea ice concentrations were obtained from the SSMR and SSM/I 25-km sea ice concentration datasets provided by the National Snow and Ice Data Center. The 200-km resolution values were determined in the same manner as the SSTs. The sea ice concentration data is initialized and updated in the model at the same time as the SSTs.

The cloud fraction in each grid cell determined the horizontal locations where water vapor is to be added and subtracted. If the cloud fraction for a specific grid cell was 50% or greater, then that grid cell was taken to be cloudy; otherwise it was considered clear. Determining the location of a given cloud in the vertical is not quite as straightforward. The cloud-top pressure from the APP-x dataset was converted to a cloud-top sigma level using 50 mb as the pressure value at the top of each column and the surface pressure for a given grid cell from the ECMWF analysis. The following pressure to sigma (σ) coordinates conversion was used:

$$\sigma = \frac{P - P_{\text{top}}}{P_{\text{sfc}} - P_{\text{top}}}, \tag{2}$$

where P is the cloud-top pressure, P_{sfc} is the surface pressure, and P_{top} is the pressure at the top of the highest model level. The calculated cloud top sigma level is then matched to the closest model sigma level, and the geopotential height at the cloud top is taken to be the geopotential height of the ECMWF analysis at that sigma level. The cloud base is then determined by subtracting the geometric cloud thickness based on the APP-x cloud properties from the geopotential height at the cloud top. The geopotential height in the ECMWF analysis that most closely matches the calculated geopotential height at the cloud base is found, and the sigma value at that model level is taken as the cloud base sigma level. The base of any cloud that was found to extend to below the surface was reset to the 0.99 sigma level. All sigma levels including and between the cloud base and the cloud top were flagged so that at the appropriate model time water vapor would be added to those levels, if a cloud is not already present in the model. Next, all grid cells that were determined to be ''clear'' based on the satellite data were checked for the presence of clouds. If a cloud was present in the model, then water vapor was subtracted. Only the model water vapor fields are altered. The ECMWF water vapor fields are only used to initialize the model and to force the lateral boundaries.

ECMWF analyses interpolated to the ARCSyM grid were obtained for 0000 and 1200 UTC for all of 1987. The ECMWF data was then linearly interpolated in time so that an analysis was available every 3 h beginning at 0000 UTC and ending at 2100 UTC. The model water vapor fields within the regions of the domain that were within 1.5 h of either APP-x composite time were updated along with the domain boundaries every 3 h. In order to force the model with the APP-x data, water vapor was simply added (subtracted) at the appropriate sigma levels where clouds (clear sky) were indicated in

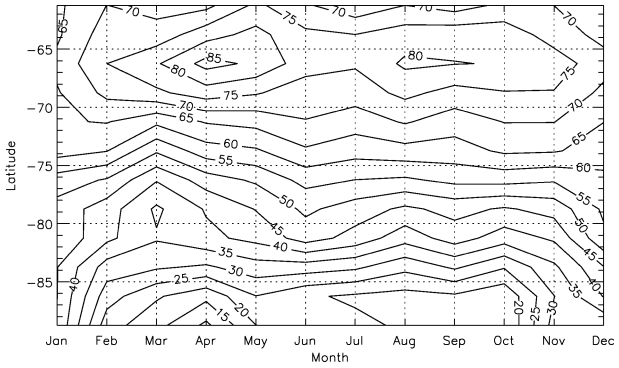

FIG. 2. The spatial and temporal distribution of mean monthly cloud amount (%) from ARCSyM experiments that incorporate the APP-x data in the Antarctic (1987).

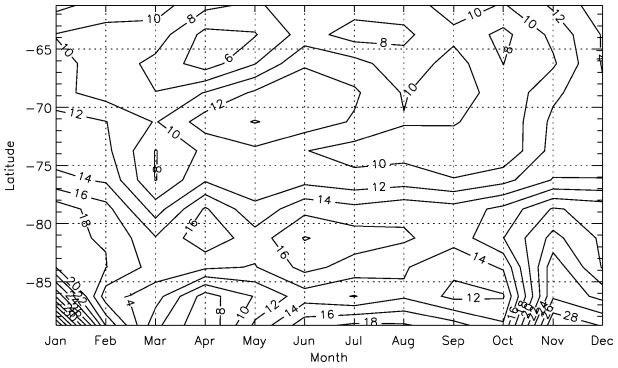

FIG. 3. The spatial and temporal distribution of the difference in mean monthly cloud amount (%) between the two types of ARCSyM experiments performed in the Antarctic (1987). The data is expressed as results with the APP-x data minus results without the APP-x data.

the APP-x data. Using an implicit moisture scheme, enough water vapor was added to make the air slightly supersaturated [relative humidity (RH) = 101%] if a cloud was indicated by the APP-x data. If clear sky was indicated by the satellite data, water vapor was subtracted so that the air was sufficiently below saturation (RH = 80%). The latent heat release associated with forcing net condensation or net evaporation in the model should have little impact on the results. This is especially true in the absolutely dry Antarctic atmosphere. In order to determine the effect of changing water vapor amounts alone on the longwave radiative fluxes, calculations were performed using the radiative transfer model, Streamer (Key and Schweiger 1998). Streamer was used because it should provide more accurate radiation calculations than the radiation package used in the ARCSyM. Longwave heating rates were calculated for clear-sky conditions (using a radiosonde profile taken over the Antarctic continent) for scenes with an ice cloud of varying optical depth for which the water vapor amounts were not altered from the original profile and for the aforementioned cloudy scenes, with the exception that each layer for which the cloud was present was saturated with respect to liquid water. The results indicate that the longwave heating due to the presence of the cloud is much greater than that associated with the larger water vapor amounts. The longwave heating rate differed by no more than 0.39 K day^{-1} under cloudy conditions when additional water vapor was added in the cloudy layers compared to when the water vapor was not altered under those same cloudy conditions. The addition of a cloud layer alone can change the longwave heating rate by more than 10 K day^{-1}, as can the elimination of a cloud. Thus, any change in the longwave heating rate profile due to changes in water vapor alone will be much smaller compared to the changes caused by clouds.

All model integrations were 48 h, and information from the APP-x dataset is used to update the model moisture fields throughout the entire 48-h period. A model ''spinup'' was allowed for by discarding the first 24 h of output and keeping only the second 24 h of output. This spinup time is consistent with the approach of Bromwich et al. (2001), Cassano et al. (2001), and Guo et al. (2003). Cloud spinup is most problematic for atmospheric models immediately after initialization, so it is more useful to evaluate a cloud assimilation scheme using short forecasts. Our goal in conducting a 1-yr series of forecast-mode simulations is to evaluate changes in errors in the modeled cloud fields over a full annual cycle. Daily means were then computed from 0000, 0600, 1200, and 1800 UTC model output. Monthly means were computed from the daily means.

4. Results

Figure 2 shows the zonally averaged spatial and monthly averaged temporal cloud amount for model runs forced with the APP-x data (the APP-x case/run) for the year 1987. Figure 3 depicts the cloud amount difference between the APP-x case and the baseline case (i.e., no APP-x data). In general, the greatest differences are found poleward of about 73°S, with the baseline run always having the lower cloud amount. This region is primarily over the Antarctic continent. During the summer, the cloud amount from the APP-x run can be as much as 40% greater than the baseline run near the pole. Throughout the entire domain, the zonally averaged cloud amount from the APP-x run is at least 4% greater than the cloud amount from the baseline run. As will be shown later, the higher cloud amount solution has more realistic values for the downwelling longwave flux at the surface. The baseline run cloud amount is up to 15% greater than the APP-x run for some grid cells, especially over the ocean (not shown). Overall, however, cloud amount from the APP-x run is larger than the baseline run, with differences up to 55%. The greatest differences tend to occur between 60° and 90°W longitude, which includes most of the Antarctic Peninsula, throughout the course of the year. This is also where, on average, the largest difference between the baseline

TABLE 1. Names and locations of automated weather stations where turbulent heat flux estimates are available. Data from the weather stations were used to construct spatially averaged sensible and latent heat estimates over the Ross Ice Shelf.

Station name	Station lat	Station lon
Marilyn	79.95°S	165.13°E
Schwerdtfeger	79.90°S	169.97°E
Gill	79.99°S	178.61°W
Lettau	82.52°S	174.45°W
Elaine	83.13°S	174.17°E
Martha II	78.38°S	173.42°W

model run cloud amounts and the actual APP-x cloud amounts are seen.

In order to determine which components of the surface energy budget are most sensitive to the induced changes in cloud cover and to assess the validity of the model output, the radiative and turbulent heat fluxes were compared to surface measurements. The radiative fluxes are compared to measurements taken at Amundsen–Scott South Pole Station for the year 1987. The measurements at the South Pole were taken by Dutton et al. (1989) from April 1986 to February 1988. The approximate absolute errors in the measurements are 2% for the shortwave and 5% for the longwave. The South Pole measurements were compared to the average of the four model grid points that surround the pole. Estimates of the sensible and latent heat fluxes at the surface over the Ross Ice Shelf by Stearns and Weidner (1993) were used to determine the validity of the turbulent heat fluxes. The sensible and latent heat flux estimates were averaged over the time period 1984–90 since a significant amount of monthly mean data for a given station and year may be missing. In addition, an area average was computed based on data from the six automated weather stations listed in Table 1. This alleviates the problem of rapidly varying surface properties when comparing a point measurement to values within the 200-km ARCSyM grid cell.

Figure 4 shows the downwelling longwave flux comparisons at the South Pole. The APP-x model runs show a positive improvement from the baseline runs every month of the year. The improvements, however, are only large during the summer months when the cloud amount from the APP-x model runs is as much as 40% greater than the cloud amount from the baseline runs. For instance, the downwelling longwave flux from the APP-x model run is about 30 W m^{-2} closer to the surface measurements than the baseline model output in January. From March to October, the downwelling longwave radiation is underestimated by as much as 23 W m^{-2} in the APP-x and baseline cases, which is similar to the errors found by King and Connolley (1997) in the U.K. Met Office Unified Climate Model, but much less than the errors found by Hines et al. (1999) with the MRF Model. The actual APP-x downwelling longwave flux also tends to be underestimated during the winter (Pavolonis 2002). This error is most likely due to a combination of clear-sky radiation and cloud cover. For all other months, the downwelling longwave flux from the APP-x model run is within the measurement error. The APP-x results show an average improvement of about 7 W m^{-2} over the baseline results throughout the year.

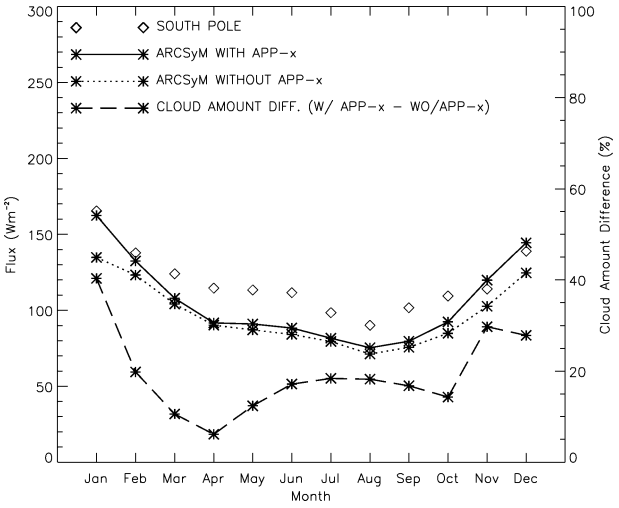

FIG. 4. The downwelling longwave radiative flux at the surface during 1987 from both model experiments compared with South Pole station measurements. The difference in cloud amount from the APP-x and baseline runs at the South Pole is also shown.

These results suggest that the incorporation of the satellite-derived data helps improve the modeled cloud cover. It should also be noted that Bailey and Lynch (2000b) found that the downwelling longwave flux from a 100-km ARCSyM experiment tended to be overestimated most of the year at the South Pole, which suggests that the cloud amount is overestimated in the ARCSyM. Our results imply that cloud amount is underestimated at the South Pole. The likely reason for these differences is the difference in model integration time. Bailey and Lynch (2000b) ran the model for 14 consecutive months using an implicit moisture scheme, whereas our model integration time was only 48 h. If we increase the model integration time to 1 month, the cloud amount increases significantly compared to results produced from just 48 h of model run time. This shows that a spinup time is needed before greater cloud coverage is seen. Thus satellite data can be used to shorten this spinup time and may be useful in model initialization for short duration forecasts.

The surface absorbed (net) shortwave radiation at the South Pole (Fig. 5) does not show an improvement with the incorporation of the APP-x data in January and November, even though the downwelling longwave radiation is significantly better during those months. This may suggest that the earth–atmosphere albedo is too large at that time because the surface-absorbed shortwave radiation is underestimated by up to 13 W m^{-2}. Also, the shortwave cooling effect of clouds is more

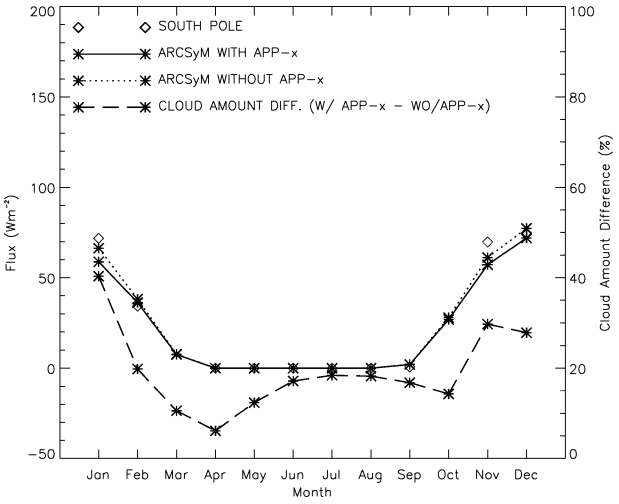

FIG. 5. The shortwave radiative flux absorbed by the surface during 1987 from both model experiments compared with South Pole station measurements. The difference in cloud amount from the APP-x and baseline runs at the South Pole is also shown.

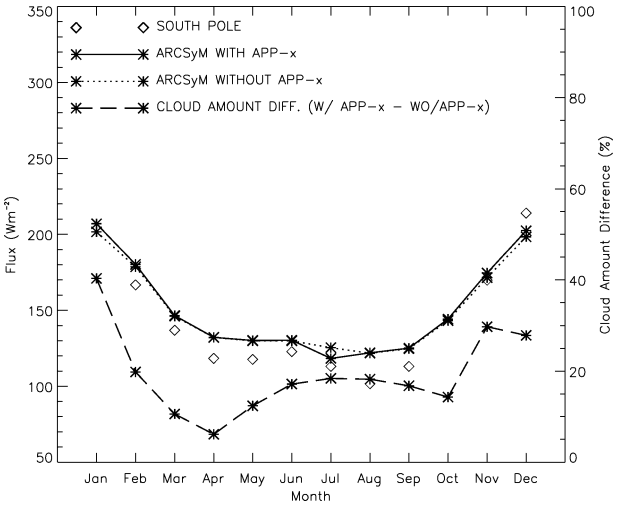

FIG. 6. The upwelling longwave radiative flux at the surface during 1987 from both model experiments compared with South Pole station measurements. The difference in cloud amount from the APP-x and baseline runs at the South Pole is also shown.

sensitive to changes in cloud optical depth than the longwave warming effect (Pavolonis and Key 2003), so it is possible that the monthly average cloud optical thickness near the South Pole may be slightly overestimated during the summer.

The upwelling longwave flux at the South Pole is shown in Fig. 6. The differences between the APP-x case and the baseline case are generally small. One may then conclude that the response of the surface temperature to changes in the downwelling longwave radiation and net shortwave radiation and net shortwave radiation are small for these 48-h model integrations. If the model integrations were longer, the differences in surface temperature between the APP-x run and the baseline run would likely be greater.

In Fig. 7, the comparisons between the sensible heat flux estimates from Stearns and Weidner (1993) and the modeled results are shown. The results that include the APP-x data compare slightly more favorably with the estimates of sensible heat flux than those for the baseline case 7 months out of the year. When the baseline case compares more favorably, the differences between the two results are still fairly small. The average difference between the model results and the station estimates are 5.8 W m^{-2} for the baseline case and 5.6 W m^{-2} for the APP-x case. As mentioned earlier, the response of surface temperature to a change in the downwelling longwave radiation and the absorbed shortwave radiation is fairly small in the 48-h integrations. This also seems to be reflected in the sensible heat flux, so the two model runs produce similar results.

Figure 8 shows the latent heat flux comparisons. As for the sensible heat flux, the differences between the APP-x case and the baseline case are small. The average error for both types of simulations is about 3 W m^{-2}, with the greatest errors occurring during the summer months. In the winter, the magnitude of the latent heat flux over the Ross Ice Shelf is a negligible component of the surface energy budget.

5. Conclusions

A method of utilizing cloud properties derived from satellite data to improve the performance of an atmospheric model was presented. Water vapor amounts in the atmospheric component of the ARCSyM were adjusted during the simulations such that the horizontal

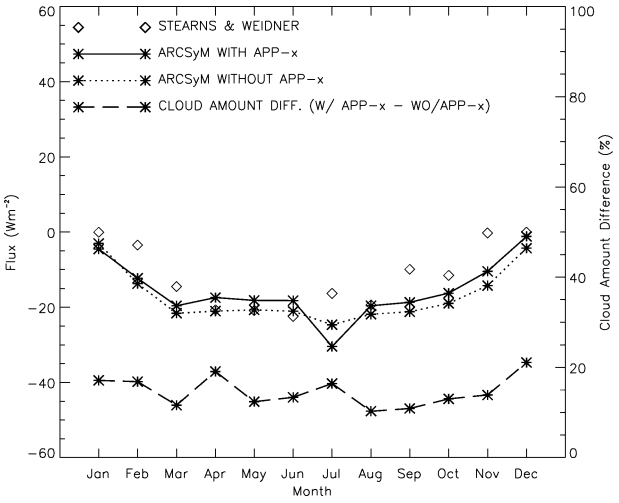

FIG. 7. The sensible heat flux at the surface from both model experiments compared with the average sensible heat flux estimated from data from automated weather station data on the Ross Ice Shelf. All modeled fluxes are for 1987 and the sensible heat flux estimates are averages based on data from 1984 to 1990. The difference in cloud amount from the APP-x and baseline runs over the Ross Ice Shelf is also shown.

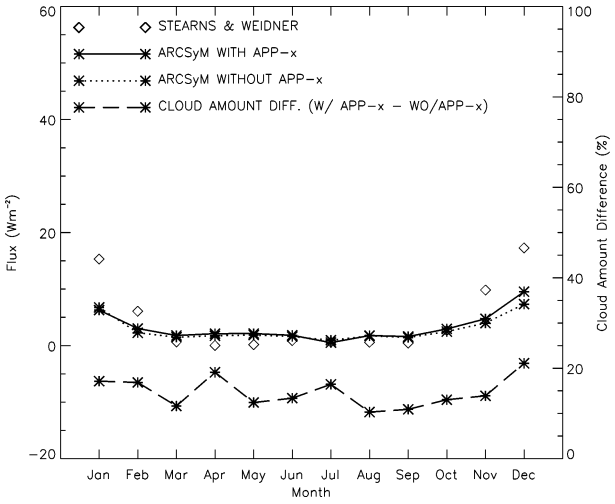

FIG. 8. The latent heat flux at the surface from both model experiments compared with the average latent heat flux estimated from several automated weather station data on the Ross Ice Shelf. Modeled fluxes are for 1987 and the latent heat flux estimates are averages based on data from 1984 to 1990. The difference in cloud amount from the APP-x and baseline runs over the Ross Ice Shelf is also shown.

and vertical location of clouds in the model more closely matched those in the APP-x satellite-based dataset. Surface radiative and turbulent heat fluxes from the model experiments were compared to measurements at the South Pole and over the Ross Ice Shelf. When the cloud fields in the ARCSyM were altered using information from the APP-x dataset, significant improvements in the monthly mean downwelling longwave radiation at the surface were observed. In the austral summer, improvements as large as 30 W m^{-2} at the South Pole, compared to the baseline results without satellite data, were seen. However, only a small improvement was seen in the turbulent heat fluxes and the surface temperature. This is probably because the model integration time of 48 h was not long enough to allow the air and surface temperature to respond appreciably to large changes in the downwelling longwave radiation.

Further improvements would be expected with better temporal coverage of the satellite data. With the APP-x dataset, which is a composite for two local solar times each day, water vapor was altered every 3 h for only portions of the domain. The results may be improved if the entire domain was updated every 3 h. In addition, the APP-x data might have a stronger impact if the cloud amount threshold used to determine if a particular model grid cell is cloudy or clear was lowered from its present value of 50%. Additionally, it is possible that the modeled atmospheric and surface temperature would be more heavily influenced by changes in the downwelling longwave flux if the model integration time was extended from 48 to 72 h or more. However, it was also found that the satellite data can be used to shorten the ''spinup'' time needed to generate a reasonable cloud field and may be useful in model initialization for short duration forecasts. Also, future model simulations should include the use of a higher horizontal and vertical spatial resolution model grid than was used in this study. Higher-resolution simulations can potentially be useful for improving the modeling of smaller-scale dynamic features such katabatic flows, which will influence the turbulent heat fluxes and hence the surface energy budget.

The chosen implicit moisture scheme has difficulty generating cloud cover over the interior of the Antarctic continent. This is evident by the fact that the simulated cloud amounts are significantly underestimated throughout the long polar winter even though the APP-x cloud amounts appear to be overestimated during this same time. For instance, the difference between the actual APP-x cloud amounts and the model cloud amounts (when the APP-x data is used to modify the model moisture fields) can exceed 50% during this time near the South Pole. However, the APP-x cloud amounts near the South Pole may, in part, be larger than the surface observations during the polar night simply because the cloud mask algorithm is detecting suspended ice crystals that cannot be seen by an observer on the ground.

In order to properly judge the performance of the model physics, each component of the surface energy budget should be carefully examined. A large source of error in atmospheric models can often be attributed to the poor simulation of cloud cover. Satellites provide an effective means of assessing cloud properties with high spatial and temporal resolution. It was shown that cloud properties from a satellite-derived dataset can be used to improve the simulation of surface energy budget components in an atmospheric model, effectively reducing one of the largest sources of error in models.

Acknowledgments. We would like to thank Bill Raymond, Bob Aune, and Jim Jung for insightful discussions. Xuanji Wang assisted with the development of the APP-x product. The standard APP development project was lead by James Maslanik and Chuck Fowler. Amanda Lynch and Elizabeth Cassano provided the ARCSyM. APP data were provided by the National Snow and Ice Data Center. This research was supported by NSF Grant OPP-0096085.

REFERENCES

Arakawa, A., and V. R. Lamb, 1977: Computational design of the basic dynamical process of the UCLA general circulation model. *General Circulation Models of the Atmosphere,* J. Chang, Ed., Methods in computational Physics, Vol. 17, Academic Press, 173–265.

Bailey, D. A., and A. H. Lynch, 2000a: Development of an Antarctic regional climate system model. Part I: Sea ice and large scale circulation. *J. Climate,* **13,** 1337–1350.

——, and ——, 2000b: Development of an Antarctic regional climate system mode. Part II: Station validation and surface energy balance. *J. Climate,* **13,** 1351–1361.

Bonan, G. B., 1996: A land surface model (LSM Version 1.0) for

ecological, hydrological, and atmospheric studies: Technical description and user's guide. NCAR Tech. Note NCAR/TN-417_STR, 150 pp.

Briegleb, B. P., 1992: Delta eddington approximation for solar radiation in the NCAR Community Climate Model. *J. Geophys. Res.*, **97,** 7603–7612.

Bromwich, D. H., J. J. Cassano, T. Klein, G. Heinemann, K. M. Hines, K. Steffen, and J. E. Box, 2001: Mesoscale modeling of katabatic winds over Greenland with the Polar MM5. *Mon. Wea. Rev.*, **129,** 2290–2309.

Cassano, J. J., J. E. Box, D. H. Bromwich, L. Li, and K. Steffen, 2001: Evaluation of Polar MM5 simulations of Greenland's atmospheric circulation. *J. Geophys. Res.*, **106,** 33 867–33 889.

Comiso, J., cited 2002: Bootstrap sea ice concentrations from Nimbus-7 SMMR and DMSP SSM/I. National Snow and Ice Data Center. [Available online at http://nsidc.org/data/docs/daac/nsidc0079_bootstrap_seaice.gd.html.]

Dutton, E. G., R. S. Stone, and J. J. DeLuisi, 1989: South Pole surface radiation balance measurements, April 1986 to February 1988. NOAA Data Rep. ERL ARL-17, 49 pp.

Giorgi, F., M. R. Marinucci, and G. T. Bates, 1993a: Development of a second generation regional climate model (RegCM2). Part I: Boundary-layer and radiative transfer processes. *Mon. Wea. Rev.*, **121,** 2794–2812.

——, ——, and ——, 1993b: Development of a second generation regional climate model (RegCM2). Part II: Convective processes and assimilation of lateral boundary conditions. *Mon. Wea. Rev.*, **121,** 2814–2832.

Gultepe, I., G. Isaac, J. Key, T. Uttal, J. Intrieri, D. Starr, and K. Strawbridge, 2003: Dynamical and microphysical characteristics of Arctic clouds using integrated observations collected over SHEBA during the April 1998 FIRE-ACE flights of the Canadian Convair. *Meteor. Atmos. Phys.*, in press.

Guo, Z., D. H. Bromwich, and J. J. Cassano, 2003: Evaluation of Polar MM5 simulations of Antarctic atmospheric circulation. *Mon. Wea. Rev.*, **131,** 384–411.

Hines, K. M., D. H. Bromwich, and R. I. Cullather, 1997: Evaluating moist physics for Antarctic mesoscale simulations. *Ann. Glaciol.*, **25,** 282–286.

——, R. W. Grumbine, D. H. Bromwich, and R. I. Cullather, 1999: Surface energy balance of the NCEP MRF and NCEP–NCAR reanalysis in Antarctic latitudes during FROST. *Wea. Forecasting,* **14,** 851–866.

Holtslag, A. A. M., E. I. F. Debruijn, and H. L. Pan, 1990: A high resolution air mass transformation model for short-range weather forecasting. *Mon. Wea. Rev.*, **118,** 1561–1575.

Hsie, E. Y., R. A. Anthes, and D. Keyser, 1984: Numerical simulation of frontogenesis in a moist atmosphere. *J. Atmos. Sci.,* **41,** 2581–2594.

Key, J. R., and A. J. Schweiger, 1998: Tools for atmospheric radiative transfer: Streamer and FluxNet. *Comput. Geosci.,* **24,** 443–451.

——, and J. Intrieri, 2000: Cloud particle phase determination with the AVHRR. *J. Appl. Meteor.,* **39,** 1797–1805.

——, X. Wang, J. Strove, and C. Fowler, 2001: Estimating the cloudy sky albedo of sea ice and snow from space. *J. Geophys. Res.*, **106** (D12), 12 489–12 497.

King, J. C., and W. M. Connolley, 1997: Validation of the surface energy balance over the Antarctic ice sheets in the U. K. Meteorological Office Unified Climate Model. *J. Climate*, **10,** 1273–1287.

Lubin, D., B. Chen, D. H. Bromwich, R. C. J. Somerville, W. Lee, and K. M. Hines, 1998: The impact of Antarctic cloud radiative properties on a GCM climate simulation. *J. Climate,* **11,** 447–462.

Lynch, A. H., W. L. Chapman, J. E. Walsh, and G. Weller, 1995: Development of a regional climate model of the western Arctic. *J. Climate,* **8,** 1555–1570.

Maslanik, J. A., C. W. Fowler, J. R. Key, T. Scambos, T. Hutchinson, and W. Emery, 1998: AVHRR-based Polar Pathfinder products for modeling applications. *Ann. Glaciol.,* **25,** 388–392.

——, A. Lynch, and C. Fowler, 1999: Assessing 2-D and coupled-model simulations of sea ice anomalies using remotely-sensed polar pathfinder products. Preprints, *Fifth Conf. on Polar Meteorology and Oceanography,* Dallas, TX, Amer. Meteor. Soc., 476–479.

Meier, W. N., J. A. Maslanik, J. R. Key, and C. W. Fowler, 1997: Multiparameter AVHRR-derived products for Arctic climate studies. *Earth Interactions,* **1.** [Available online at http://EarthInteractions.org.]

Mlawer, E. J., S. J. Taubman, P. D. Brown, M. J. Iacono, and S. A. Clough, 1997: Radiative transfer for inhomogeneous atmospheres: RRTM, a validated correlated-K model for the longwave. *J. Geophys. Res.,* **102** (D14), 16 663–16 682.

Parkinson, C. L., and W. M. Washington, 1979: A large-scale numerical model of sea-ice. *J. Geophys. Res.,* **84,** 311–337.

Pavolonis, M. J., 2002: Antarctic cloud radiative forcing at the surface estimated from the ISCCP D1 and AVHRR Polar Pathfinder data sets, 1985–1993. M.S. thesis, Dept. of Atmospheric and Oceanic Sciences, University of Wisconsin—Madison, 123 pp.

——, and J. R. Key, 2003: Antarctic cloud radiative forcing at the surface estimated from the AVHRR Polar Pathfinder and ISCCP D1 data sets, 1985–1993. *J. Appl. Meteor.,* **42,** 827–840.

Schramm, J. L., M. Holland, J. A. Curry, and E. E. Ebert, 1997: Modeling the thermodynamics of a distribution of sea ice thickness. Part I: Sensitivity to ice thickness resolution. *J. Geophys. Res.,* **102,** 23 079–23 092.

Stearns, C. R., and G. A. Weidner, 1993: Sensible and latent heat flux estimates in Antarctica. *Antarctic Meteorology and Climatology: Studies Based on Automated Weather Stations,* D. H. Bromwich and C. R. Stearns, Eds., Antarctic Research Series, Vol. 61, Amer. Geophys. Union, 109–138.

Trenberth, K. E., 1992: Global analyses from ECMWF and atlas of 1000 to 10 mb circulation statistics. NCAR Tech. Note TN-373 + STR, 191 pp.